Fast Bayesian inference of optical trap stiffness and particle friction

Sudipta Bera†,[1] Shuvojit Paul†,[1] Dipanjan Ghosh,[2] Avijit Kundu,[1] R. Adhikari,[3] and Ayan Banerjee[1]

[1] *Dept of Physical Sciences, Indian Institute of Science Education and Research, Kolkata, Mohanpur 741246*

[2] *Dept of Chemical Engineering, Jadavpur University, Kolkata 700032*

[3] *The Institute of Mathematical Sciences, CIT Campus, Taramani, Chennai 600113**

(Dated:)

Bayesian inference provides a principled way of estimating the parameters of a stochastic process that is observed discretely in time. The overdamped Brownian motion of a particle confined in an optical trap is generally modelled by the Ornstein-Uhlenbeck process and can be observed directly in experiment. Here we present Bayesian methods for inferring the parameters of this process, the trap stiffness and the particle friction coefficient, that use exact likelihoods and sufficient statistics to arrive at simple expressions for the maximum a posteriori estimates. This obviates the need for Monte Carlo sampling and yields methods that are both fast and accurate. We apply these to experimental data and demonstrate their advantage over commonly used non-Bayesian fitting methods.

I. INTRODUCTION

Since the seminal contributions of Rayleigh, Einstein, Smoluchowki, Langevin and others [1], stochastic processes have been used to model physical phenomena in which fluctuations play an essential role. Examples include the Brownian motion of a particle, the fluctuation of current in a resistor, and the radioactive decay of subatomic particles [2]. A central problem is to infer the parameters of the process from partially observed sample paths, for instance, the diffusion constant from a time series of positions, or the resistance from a time series of current measurements, and so on. Bayesian inference provides a principled solution to this inverse problem [3], making optimal use of the information contained in the partially observed sample path [4].

The sample path of a harmonically confined Brownian particle is usually modelled by the Ornstein-Uhlenbeck process [2, 5]. This process has a mean regression rate λ and a volatility σ which map, in the physical application, to the stiffness k of the harmonic potential, the friction γ of the particle and the temperature k_BT of the ambient fluid. Since the friction of a particle of radius a is given by $\gamma = 6\pi\eta a$, where η is the viscosity of the fluid, any estimation of the friction also provides an estimate of the viscosity of the medium, given the particle radius. Thus, the viscosity, which is defined as the macroscopic response of the fluid to an externally imposed shear, can be inferred from microscopic obversation of the Brownian fluctuations of harmonically confined particle. Likewise, the particle diffusion coefficient D can be inferred from the friction through the Einstein relation $D = k_BT/\gamma$. These, of course, are consequences of the relation between response and correlation that prevails in a physical system in thermal equilibrium [6].

In this paper, we apply Bayesian inference to the problem of estimating the parameters of an optically trapped Brownian sphere from time series that represent partially observed sample paths, under conditions in which these paths can be modelled as an Ornstein-Uhlenbeck process. This is of great current experimental relevance, since harmonic confinement of micron-sized spheres is ubiquitous in optical tweezers. A reliable estimation of the trap stiffness is a necessary first step in using tweezers for force measurements. Reliable estimate of the particle friction is immediately useful in microrheology. A Bayesian method Monte Carlo sampling has been proposed earlier to this end [7]. Here, we present two Bayesian methods that do away with sampling by exploiting the exact likelihoods and sufficient statistics of the problem and provide thereby, *exact* maximum a posteriori parameter estimates in terms of these statistics. Consequently, both methods are extremely fast and accurate, and are able to estimate the trap stiffness or the particle friction from a time series with a million points in less than a millisecond. Further, the fluctuation-dissipation relation provides provides a stringent internal consistency check on the accuracy of estimation of the trap stiffness from each of these methods. We apply both methods to experimental data to obtain estimates that have excellent internal consistency. These estimates are found to be in good agreement with commonly used non-Bayesian calibration methods [8]. We discuss the advantages of our methods in comparision to standard calibriation methods in optical tweezer experiments. The remainder of the paper is organized as follows. In the next section we recall several key properties of the sample paths and distributions of the Ornstein-Uhlenbeck process. In Section III, we present the Bayesian methods, in section IV we describe the experimental setup, and in section V we apply the Bayesian procedures to the experimental data. We conclude with a discussion of future directions in Bayesian inference in optical tweezer experiments while advocating its use as a complement to standard fitting methods.

* rjoy@imsc.res.in

II. ORNSTEIN-UHLENBECK PROCESS

The Langevin equation for a Brownian particle confined in a potential U is given by

$$m\dot{v} + \gamma v + \nabla U = \xi \tag{1}$$

where $\xi(t)$ is a zero-mean Gaussian white noise with variance $\langle \xi(t)\xi(t')\rangle = 2k_BT\gamma\delta(t-t')$ as required by the fluctuation-dissipation theorem. In the limit of vanishing inertia and a harmonic potential, $U = \frac{1}{2}kx^2$, we obtain the overdamped Langevin equation

$$\dot{x} = -\frac{k}{\gamma}x + \sqrt{\frac{2k_BT}{\gamma}}\zeta(t) \tag{2}$$

where $\zeta(t)$ is now a zero-mean Gaussian white noise with unit variance. This is the Ornstein-Uhlenbeck process, whose sample paths obey the Ito stochastic differential equation [5],

$$dx = -\lambda x dt + \sigma dW \tag{3}$$

where W is the Wiener process, $\lambda = k/\gamma$ is the mean-regression rate and $\sigma = \sqrt{2k_BT\gamma^{-1}}$ is the volatility. Since $D = k_BT\gamma^{-1}$ we have $\sigma^2 = 2D$. In problems involving Brownian motion, it is convenient to work with the diffusion coefficient, rather than the volatility, and therefore we infer D, rather than σ, directly.

The transition probability density $P_{1|1}(x't'|x\,t)$, the probability of a displacement from x at time t to x' at time t', obeys the Fokker-Planck equation $\partial_t P_{1|1} = \mathcal{L}P_{1|1}$, where the Fokker-Planck operator is

$$\mathcal{L} = \frac{\partial}{\partial x}\lambda x + \frac{\partial^2}{\partial x^2}D. \tag{4}$$

The solution is a normal distribution,

$$x't'|x\,t \sim \mathcal{N}\left(xe^{-\lambda(t'-t)}, \frac{D}{\lambda}[1-e^{-2\lambda(t'-t)}]\right), \tag{5}$$

where $\mathcal{N}(a,b)$ is the univariate normal distribution with mean a and variance b. This solution is exact and holds for arbitrary values of $|t-t'|$. The correlation function decays exponentially,

$$C(t-t') \equiv \langle x(t)x(t')\rangle = \frac{k_BT}{k}e^{-\lambda|t-t'|} \tag{6}$$

a property guaranteed by Doob's theorem for any Gauss-Markov processes [2]. The Fourier transform of the correlation function gives the power spectral density

$$C(\omega) \equiv \langle |x(\omega)|^2\rangle = \frac{k_BT}{k}\frac{1}{\omega^2+\lambda^2} \tag{7}$$

which is Lorentzian in the angular frequency ω. The relation $D/\lambda = k_BT/k$ has been used while obtaining the last two relations.

The stationary distribution $P_1(x)$ obeys the steady state Fokker-Plank equation $\mathcal{L}P_1 = 0$ and the solution is a normal distribution,

$$x \sim \mathcal{N}\left(0, \frac{D}{\lambda}\right) = \mathcal{N}\left(0, \frac{k_BT}{k}\right). \tag{8}$$

Comparing the forms of $P_{1|1}$ and P_1 it is clear that former tends to the latter for $|t-t'| \to \infty$, as it should.

III. BAYESIAN INFERENCE

Consider, now, the time series $X \equiv (x_1, x_2, \ldots, x_N)$ consisting of observations of the sample path $x(t)$ at the discrete times $t = n\Delta$t with $n = 1, \ldots, N$. Then, using the Markov property of the Ornstein-Uhlenbeck process, the probability of the sample path is given by [9]

$$P(X|\lambda, D) = \prod_{n=1}^{N-1} P_{1|1}(x_{n+1}|x_n, \lambda, D)P_1(x_1|\lambda, D) \tag{9}$$

The probability $P(\lambda, D|X)$ of the parameters, given the sample path, can now be computed using Bayes theorem, as

$$P(\lambda, D|X) = \frac{P(X|\lambda, D)P(\lambda, D)}{P(X)}$$

The denominator $P(X)$ is an unimportant normalization, independent of the parameters, that we henceforth ignore. Since both k and γ must be positive, for stability and positivity of entropy production respectively, we use informative priors for λ and D, $P(\lambda, D) = H(\lambda)H(D)$, where H is the Heaviside step function. This assigns zero probability weight for negative values of the parameters and equal probability weight for all positive values. The logarithm of the posterior probability, after using the explicit forms of $P_{1|1}$ and P_1, is

$$\begin{aligned}\ln P(\lambda, D|X) = \frac{N-1}{2}\ln\frac{\lambda}{2\pi DI_2} - \frac{\lambda}{2DI_2}\sum \Delta_n^2 \\ + \frac{1}{2}\ln\frac{\lambda}{2\pi D} - \frac{\lambda}{2D}x_1^2\end{aligned} \tag{10}$$

where we have defined the two quantities

$$I_2 \equiv 1 - e^{-2\lambda\Delta t}, \quad \Delta_n \equiv x_{n+1} - e^{-\lambda\Delta t}x_n$$

and the sum runs from $n = 1, \ldots, N-1$.

The maximum a posteriori (MAP) estimate $(\lambda^\star, D^\star)$ solves the stationary conditions $\partial \ln P(\lambda, D|X)/\partial\lambda = 0$ and $\partial \ln P(\lambda, D|X)/\partial D = 0$, while the error bars of this estimate are obtained from the Hessian matrix of second derivatives evaluated at the maximum [3, 10, 11]. The

analytical solution of the stationary conditions, derived in the Appendix, yields the MAP estimate to be

$$\lambda^\star = \frac{1}{\Delta t} \ln \frac{\sum x_n^2}{\sum x_{n+1} x_n}$$
$$D^\star = \frac{\lambda^\star}{N} \left(\frac{\sum \Delta_n^2}{I_2} + x_1^2 \right)$$
$$\frac{k^\star}{k_B T} = \frac{\lambda^\star}{D^\star} \tag{11}$$

where both I_2 and Δ_n are now evaluated at $\lambda = \lambda^\star$. These provide direct estimates of the parameters *without* the need for fitting or sampling. The errors bars of these estimates are obtained from the matrix of second derivates of the posterior, evaluated at the maximum. We do not provide their unwieldy expressions but do make use of them when reporting errors of the MAP estimates obtained from experimental data (see below). We refer to this procedure as "Bayes I" below.

A second Bayesian procedure for estimating the trap stiffness directly results when X is interpreted not as a time series but as an exchangeable sequence, or, in physical terms, as repeated independent observations of the stationary distribution $P_1(x)$ [10]. In that case, the posterior probability, assuming an informative prior that constrains k to positive values, is

$$\ln P(k|X) = \frac{N}{2} \ln \frac{k}{2\pi k_B T} - \frac{1}{2} \frac{k}{k_B T} \sum_{n=1}^{N} x_n^2 \quad (k > 0) \tag{12}$$

The MAP estimate and its error bar follow straightforwardly from the posterior distribution as

$$\frac{k^\star}{k_B T} = \frac{N}{\sum_{n=1}^{N} x_n^2}, \quad \sigma_{k^\star} = \frac{1}{\sqrt{N}} \frac{k^\star}{k_B T} \tag{13}$$

and, not unexpectedly, the standard error decreases with increasing number of sampling points. This procedure is independent of the sampling rate and is equivalent to the equipartition method when the Heaviside prior is used for k. We refer to this procedure as "Bayes II" below.

A comparison of the estimates for the trap stiffness obtained from these independent procedures provides a check on the validity of the Ornstein-Uhlenbeck process as a data model. Any significant disagreement between the estimates from the two methods signals a breakdown of the applicability of the model and the assumptions implicit in it: overdamped dynamics, constant friction, harmonicity of the potential, and thermal equilibrium.

The posterior probabilities in both methods can be written in terms of four functions of the data

$$T_1(X) = \sum x_{n+1}^2, \quad T_2(X) = \sum x_{n+1} x_n,$$
$$T_3(X) = \sum x_n^2, \quad T_4(X) = x_1^2, \tag{14}$$

which, therefore, are the sufficient statistics of the problem. The *entire* information in the time series X relevant to estimation is contained in these four statistics [10]. Their use reduces computational expense enormously, as only four numbers, rather than the entire time series, are required. The combined use of exact likelihoods, sufficient statistics and analytical MAP estimates yields fast and accurate methods for estimating parameters from the time series of particle positions. This completes our description of the Bayesian procedure for jointly estimating λ and D, and from there, γ and k.

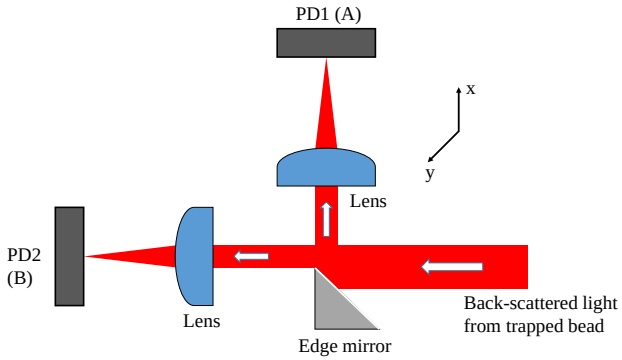

Figure 1. Schematic of balanced detection scheme to measure Brownian motion in the x direction from a single trapped polystyrene sphere. Back-scattered light from the trapped sphere is incident on an edge mirror that divides it equally between photodiodes PD1 and PD2, having voltage outputs A and B respectively. The normalized x coordinate of the sphere at any instant in time is given by $(A-B)/(A+B)$.

IV. EXPERIMENTAL SETUP AND DATA ACQUISITION

We collect position fluctuation data of an optically trapped Brownian particle using a standard optical tweezers setup that is described in detail in [13]. Here we provide a brief overview. The optical tweezers system is constructed around a Zeiss inverted microscope (*Axiovert.A1*) with a $100x$ 1.4 numerical aperture (NA) objective lens tightly focusing laser light at 1064 nm from a semiconductor laser (*Lasever*, maximum power 500mW) into the sample. The back aperture of the objective is slightly overfilled to maximize the trapping intensity. The sample consists of a dilute suspension (volume fraction $\phi = 0.01$) of polystyrene sphere of diameter 3μm in 10% NaCl-water solution, around $20\mu l$ of which is pipetted on a standard glass cover slip. The total power available at the trapping plane is around 15 mW. The motion of a single trapped particle is observed by back-focal plane interferometry using the back-scattered intensity of a detection laser at 671 nm that co-propagates with the trapping laser. The detection laser power is maintained at much lower levels than that required to trap a particle. The back-scattered signal from the trapped particle is measured using a balanced detection scheme, schematically illustrated in Fig. 1. The back-scattered light beam

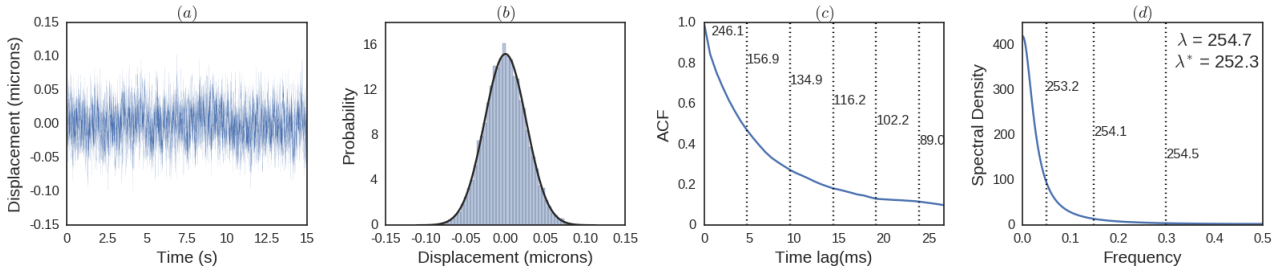

Figure 2. Discrete sample path and empirical statistics of an optically trapped 3μm Brownian polysterene bead. Panel (a) shows discrete observations of one coordinate of the sample path, (b) the histogram the coordinate, (c) the autocorrelation function and (d) the spectral density. The fit of λ from the both the autocorrelation and the spectral density vary on the amount of data used [8, 12]. The numbers alongside the vertical lines indicate values of λ fitted using data to the *left* of the corresponding line.

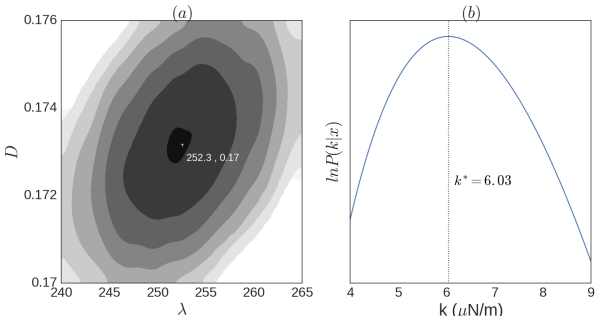

Figure 3. Logarithms of the posterior probability density for Bayes I (left) and Bayes II (right). The MAP estimate for Bayes I is shown by the + and for Bayes II by the vertical line. The error bars are obtained from the Hessian matrix of second derivatives evaluated at the MAP value.

is incident on an edge mirror which divides it equally into two halves that are focused using two lenses of equal focal length on photodiodes PD1 and PD2 (*Thorlabs* PDA100A-EC Si-photodiodes of bandwidth 2.4 MHz). The voltage outputs A and B, of PD1 and PD2 respectively, are then combined as $(A-B)/(A+B)$ to give the normalized value of the x coordinate of motion at any instant of time. The advantage of such balanced detection is that the intensity fluctuations of the laser are present in both beams simultaneously and are thus canceled out when the difference is taken. Note that the direction of the edge mirror decides whether the x or y coordinate of motion is being measured. The mirror is rotated by 90 degrees to select between the coordinates. The fast response of the photodiodes, with a rise time of 50ns at highest gain, ensures that spurious correlations are kept to a minimum and the data filtering necessary with slower commercial quadrant photodetectors is avoided entirely. The data from the photodiodes is logged into a computer using a National Instruments DAQ system and Labview at sampling rates between 2-5 kHz. For calibrating the motion, *i.e.* converting the voltage into physical distance which is necessary for measuring the diffusion constant, we employ an acousto-optic modulator that is placed in the back-focal plane of the microscope objective and scan the trapped bead by distances which are determined from the pixel calibration of images taken by the camera attached to the microscope [13]. The balanced detection output is simultaneously measured to yield the voltage-distance calibration of the detection system. For the viscosity measurement, we add glycerol to water in fixed proportions to create 5 samples of different viscosity. The viscosity of each sample is then measured by a commercial rheometer (Brookfield DB3TLVCJ0) to match with the experimental results.

We note that the final measured data is a result of a transformation by the detection apparatus of the physical sample paths. The Bayesian modelling of the detection apparatus and the transformations it induces is not pursued here but will be the focus of a future work.

V. RESULTS

In Figure. (2) we show a typical sample path of the component of motion in the plane of the trap together with its histogram, autocorrelation and spectral density. The histogram shows that stationary distribution of positions is well-approximated by a Gaussian. The variance $\langle x^2 \rangle$ is used in the conventional "equipartition" method to estimate the spring constant k, while the fitting of the autocorrelation to the exponential in Eq.(6) or of the spectral density to the Lorentzian in Eq. (7) is used to estimate the spring constant when the friction constant is assumed to be known. The considerable pitfalls in reliably estimating the spring constant from these apparently straightforward procedures have been extensively discussed in the literature. We follow well-accepted procedures in estimating the stiffness from spectral density.

The results of Bayesian inference are shown in Figure.

Laser power (mW)	k ($\mu N m^{-1}$)		
	Bayes I	Bayes II	PSD
10.1	1.10(8)	1.09(10)	1.30(10)
16.1	2.23(12)	2.23(12)	2.40(12)
27.2	3.88(15)	3.88(15)	3.99(15)
31.8	4.16(15)	4.16(15)	4.25(19)
33.6	4.48(19)	4.48(19)	4.40(25)
36.8	4.83(20)	4.83(20)	4.67(25)

Table I. Variation of trap stiffness k with laser power estimated by the two Bayesian methods of this work (Bayes I and Bayes II) and by the standard fit to the spectral density (PSD) [8]. For each value of laser power, the corresponding stiffness is the mean over 5 different sets of measurements. The variance of mean is indicated in parentheses. The Bayesian standard error is less than $\frac{1}{2}\%$ of the mean for each data set.

η	D	$D^\star$	$\eta^\star$
0.00089	1.65	1.72(6)	0.00085(3)
0.00137	1.07	1.05(3)	0.00139(4)
0.00197	0.743	0.732(11)	0.00200(3)
0.00243	0.603	0.586(12)	0.00250(5)
0.00487	0.301	0.276(14)	0.00530(8)

Table II. Bayesian viscometry in an optical trap. The first column is the viscosity of the solvent as measured in a rheometer and the second column is the diffusion coefficient as given by the Stokes-Einstein relation for that value of the viscosity. The third column is the Bayesian MAP estimate for the diffusion coefficient and the fourth column is the value of the viscosity, as given by the Stokes-Einstein relation for that value of the diffusion coefficient. There is a good match between the first and fourth columns.

(2). In panel (a) we show a heat map of the Bayesian posterior distribution in the $\lambda - D$ plane, together with contours of equal probability, for the "Bayes I" method. There is a single maximum at $(\lambda^\star, D^\star)$ whose numerically computed value is in excellent agreement with the analytical MAP estimates of Eq.(11). In panel (b) we show the Bayesian posterior distribution for the stiffness for the "Bayes II" method. There is remarkably good agreement between these two conceptually and procedurally independent Bayesian methods in estimating the stiffness, as shown in Table.(I). The agreement with the conventional method, shown in the third column, is within 10% in all cases. The typical length of our time series is $N \sim 30000$ and this gives a Bayesian standard error that is less than $\frac{1}{2}\%$ of the mean. These are well below the systematic errors and the approximately 3% variability of the estimates obtained from the fitting procedure.

To compare the Bayesian estimate for the diffusion coefficient we repeat the experiment for different solve nt viscosities keeping both the laser power and the particle size fixed. The Stokes-Einstein relation then provides an estimate of the diffusion coefficient. We compare this estimate with the MAP estimate $D^\star$ in Table. (II) to find agreement to within 10% in all cases. The Stokes-Einstein relation can be used "in reverse" to obtain a MAP estimate of the viscosity, $\eta^\star$, which agrees very well with the known viscosity of the mixture. Thus, the Bayesian method can be used for accurate viscometry using only the discretely observed sample paths of a trapped Brownian particle.

VI. DISCUSSION

- use of exact likelihood removes the need to sample at high frequencies. this is the limitation of Euler approximation used in the paper of the French group. accuracy.
- use of analytical MAP estimates removes the need for Monte Carlo sampling, speed.
- use of sufficient statistics reduces the entire time series to four numbers, efficiency.
- joint probability obtained, can marginalize out friction if that is not known and treat it as a nuisance parameter
- can do many more complicated models, e.g. air trapping etc, using Bayesian inference.

This solution is exact and holds for arbitrary values of $|t-t'|$, unlike the approximate solution used in [7], which is accurate only when $\lambda|t-t'| \ll 1$.

ACKNOWLEDGMENTS

RA gratefully acknowledges Professor M. E. Cates for introducing him to the Bayesian interpretation of probability and to Bayesian inference.

A. Appendix

The partial derivatives of the logarithm of the posterior probability with respect to λ and D are

$$\frac{\partial \ln P}{\partial \lambda} = \frac{N-1}{2}\left(\frac{1}{\lambda} - \frac{I_2'}{I_2}\right) - \frac{\sum \Delta_n^2}{2DI_2} - \frac{\lambda}{2D}\frac{\partial}{\partial \lambda}\left(\frac{\sum \Delta_n^2}{I_2}\right) + \frac{1}{2\lambda} - \frac{x_1^2}{2D}$$

$$\frac{\partial \ln P}{\partial D} = -\frac{N-1}{2D} + \frac{\lambda \sum \Delta_n^2}{2D^2 I_2} - \frac{1}{2D} + \frac{\lambda x_1^2}{2D^2},$$

where $I_2' = 2\Delta t\, e^{-2\lambda\Delta t}$. Setting the second of these equations to zero, D is solved in term of λ and this solution is used in the first equation, together with the large-sample asymptotics

$$\frac{\lambda}{N}\left(\frac{\sum\Delta_n^2}{I_2} + x_1^2\right) \approx \frac{\lambda}{(N-1)}\frac{\sum\Delta_n^2}{I_2},$$

to cancel all D-dependent terms. Setting the resulting equation to zero and solving for λ then yields the MAP estimates in Eq.(11).

- Overview of time series, histogram, autocorrelation and power spectral density - Fig. 1
- Bayesian results, joint probability plot, together with marginals - Fig. 2
- Variation of k with laser power Bayes I, Bayes II, psd (need to say that γmust be known) - Table 1
- Microrheological application - from friction to η- Table 2
- Bayes I : less sensitive to drift, does not require prior knowledge of particle radius or fluid viscosity : these are estimated from the data.
- Bayes II : more sensitive to drift, directly estimates k, consistency with Bayes I is an excellent test of implicit assumptions.
- Both methods have statistical errors that scale as inverse square root of the number of data points. With a 1000 points, the statistical accuracy would be 3% of the MAP estimate, and with 10000 points, it would be less than 1% of the MAP estimate.
- Method jointly estimates both lambda and D. PSD requires D to be known.

The results of our measurements of trap stiffness as a function of trapping laser power and the viscosity of the glycerol + water solutions are summarized in Fig. 2 and Tables I and II, respectively. For each data set of the displacement of the single trapped polystyrene bead of diameter 3μm (Brownian particle), we first check the quality of raw time series data (Fig. 2(a)) from the position histogram counts and ensure that it fits well to a Gaussian (Fig. 2(b)). We then plot the autocorrelation function (ACF) and power spectral density (PSD) of the data, and again ensure robust exponential and Lorentzian fits, respectively (Fig. 2(c) and (d)). The Bayesian analyses is carried out only for those series of data which show good results in the preliminary analyses, and we proceed to calculate the MAP estimate for $(\lambda^\star, D^\star)$ both analytically and numerically as shown in Fig. 2(e). As is clear from the figure, the results match very well, and the standard deviation of the estimated parameters for one set of time series data using the Bayesian analysis is less than 0.1%. In comparison, the corresponding error in the estimates from the PSD for a single time series data set is much higher, being typically of the order of 3-4%. This can be principally attributed to the variation in the fit parameters depending on the start and end points of the Lorentzian fit to the data shown in Fig. 2(d). Thus, it is clear that the inherent error in the Bayesian estimation is far lesser than that in the PSD fit - something which is important to note considering that the Lorentzian fit to the PSD is the most standard calibration method in optical trapping. However, we still use the PSD technique as a benchmark for our estimates of k at different trapping laser powers, which are shown in Table I. The trapping stiffness increases linearly with laser power, and we check for this by trapping at six different laser powers, with five sets of time series data used for each laser power. The measured values of k by the Bayesian MAP and stationary (equipartition) analyses agree very well. Note that the 1σ errors indicated in parenthesis are actually the standard errors of the mean values of k after averaging over the five different data sets for each laser power, and should not be confused with the inherent error in the Bayesian statistics. PSDs are also computed for the same five sets of data, and a typical averaged spectrum for the laser power of 10.1 mW is shown in Fig. 2(d). The variation of trap stiffness with laser power is shown in Fig. 2(f), and we get good linear fits with the slopes (rate of change of stiffness with laser power) of the Bayesian processes (we do not show the MAP and stationary analyses data separately since they overlap almost completely as shown in Table I) and the PSD agreeing well within 1σ. For the viscosity data, we show the values of D in Table II, from which the values of η are evaluated using the Einstein relation $\left(\eta = \frac{k_B T}{6\pi D a},\ \text{a = bead radius}\right)$. In these sets of experiments, the voltage-physical distance calibration becomes of crucial importance, and we perform fresh calibrations for each different viscosity sample. The agreement with the viscosity values measured using the rheometer is good to within 3% for all data points except for the highest viscosity value, where the trap was not very robust due to the high viscosity, with the corner frequency $\left(\frac{\lambda}{2\pi}\right)$ being rather low for the same laser power. Note that for all these measurements the trap stiffness was kept constant to around 6 $pN/\mu m$.

[1] S. Chandrasekhar, *Reviews of modern physics*, 1943, **15**, 1.

[2] N. G. Van Kampen, *Stochastic processes in physics and chemistry*, Elsevier, 1992, vol. 1.

[3] H. Jeffreys, *The theory of probability*, OUP Oxford, 1998.

[4] A. Zellner, *The American Statistician*, 1988, **42**, 278–280.
[5] C. W. Gardiner *et al.*, *Handbook of stochastic methods*, Springer Berlin, 1985, vol. 3.
[6] R. Kubo, *Reports on progress in physics*, 1966, **29**, 255.
[7] M. U. Richly, S. Türkcan, A. Le Gall, N. Fiszman, J.-B. Masson, N. Westbrook, K. Perronet and A. Alexandrou, *Optics express*, 2013, **21**, 31578–31590.
[8] K. Berg-Sørensen and H. Flyvbjerg, *Review of Scientific Instruments*, 2004, **75**, 594–612.
[9] M. C. Wang and G. E. Uhlenbeck, *Reviews of Modern Physics*, 1945, **17**, 323.
[10] E. T. Jaynes, *Probability theory: The logic of science*, Cambridge university press, 2003.
[11] D. Sivia and J. Skilling, *Data analysis: a Bayesian tutorial*, OUP Oxford, 2006.
[12] M. Tassieri, R. Evans, R. L. Warren, N. J. Bailey and J. M. Cooper, *New Journal of Physics*, 2012, **14**, 115032.
[13] S. B. Pal, A. Haldar, B. Roy and A. Banerjee, *Review of Scientific Instruments*, 2012, **83**, 023108.